Research Article Open Access

Jiaoliang Wang, Liping Long* Guing Xiao, FangFang

Reversible Fluorescent Turn-on Sensors for Fe^{3+} based on a Receptor Composed of Tri-oxygen Atoms of Amide Groups in Water

https://doi.org/10.1515/chem-2018-0140
received April 22, 2018; accepted September 12, 2018.

Abstract: Compounds **Rh6G-1** and **RhB-2** with a novel receptor composed of tri-oxygen atoms of amide groups were designed and synthesized as new reversible fluorescent sensors for Fe^{3+}. The prominent features of the novel sensor **Rh6G-1** include a large fluorescence turn-on response in essentially pure water at room temperature, high sensitivity, high selectivity, a limit of detection, cell membrane permeability, and low cytotoxicity. These desirable attributes enable us to successfully employ the new sensor **Rh6G-1** for Fe^{3+} bioimaging in living cells.

Keywords: Sensor; Reversibility; Fe^{3+}; tri-oxygen.

1 Introduction

Iron is an essential trace element with significant roles in chemical and biological processes [1]. As iron transporting, storage, and balance are tightly regulated in an organism [2], iron deficiency or overload may induce various diseases [1,3]. Thus, the detection of iron ions is highly important. Many sophisticated analytical techniques, including atomic absorption, ICP-AES, and voltammetry have been used to detect Fe^{3+} ions in environment [4-6]. However, there is a high demand to develop inexpensive and real-time monitoring methods for the detection of Fe^{3+} in biosystems.

Recently, a number of fluorescence-enhanced Fe^{3+} sensors based on reversible Fe^{3+} coordination or Fe^{3+}-mediated reactions have been reported [7-18]. However, some of them could only function in organic solvents or aqueous-organic media. This incompatibility with water may restrict their potential bio-applications. Therefore, the design of new reversible fluorescent turn-on Fe^{3+} sensors with high selectivity, high sensitivity, rapid response, and good water solubility for bio-applications remains demanding.

Herein, the choice of rhodamine derivatives as the fluorophore is based on the excellent photophysical properties of rhodamine derivatives, which have been extensively employed as a sensing platform for diverse arrays of metal ions, neutral bio-molecules (e.g. NO, HClO, Cys, etc), and anions [19-21]. Furthermore, inspired by the prior report that Fe^{3+} strongly complexes with the tri-oxygen atoms of the amide groups in the bioactive ferrichromes [22], we further select the similar tri-oxygen atoms of the amide groups as the candidate recognition unit for Fe^{3+}. To our best knowledge, this recognition unit has not been previously exploited in design of reversible fluorescent Fe^{3+} sensors. Notably, the novel recognition unit is distinct from the existing N, S, O or N, O atoms as the Fe^{3+} receptors [7].

In this work, we report the synthesis of new reversible fluorescent turn-on sensors **Rh6G-1** for Fe^{3+} in essentially pure water. The sensors of **Rh6G-1** and **RhB-2** have been synthesized in one step by condensation of rhodamine 6G/B hydrazides with excess isocyanatobenzene (PhNCO), and find that sensors **Rh6G-1**demonstrate high selectivity toward Fe^{3+} over a wide range of tested metal ions in almost pure water. More importantly, the sensor **Rh6G-1** is a reversible turn-on sensor for Fe^{3+}, and could effectively work at cellular level.

***Corresponding author: Liping Long,** Hunan Provincial Key Lab of Dark Tea and Jin-hua, College of Materials and Chemical Engineering, Hunan City University, Yiyang, Hunan 413000, China, E-mail: llping401@163.com
Jiaoliang Wang, Guing Xiao, FangFang: Hunan Provincial Key Lab of Dark Tea and Jin-hua, College of Materials and Chemical Engineering, Hunan City University, Yiyang, Hunan 413000, China

2 Materials and Methods

2.1 Materials and instruments

Unless otherwise stated, all reagents were purchased from commercial suppliers and used without further purification. Solvents used were purified by standard methods prior to use. Twice-distilled water was used throughout all experiments. The salts used in the stock solutions of metal ions were NaCl, KCl, $NiCl_2·6H_2O$, $AgNO_3$, $MnCl_2·4H_2O$, $ZnCl_2$, $MgCl_2·6H_2O$, $CaCl_2$, $CdCl_2·2.5H_2O$, $CuCl_2·2H_2O$, $FeCl_2·4H_2O$, $CoCl_2·6H_2O$, $HgCl_2$, $Pd(C_2H_3O_2)_2$, $PbCl_2$, $AuCl_3$ and $FeCl_3·6H_2O$. Melting points of compounds were measured on a Beijing Taike XT-4 microscopy melting point apparatus, all melting points were uncorrected; Low resolution mass spectra were performed using an LCQ Advantage ion trap mass spectrometer from Thermo Finnigan or Agilent 1100 HPLC/MSD spectrometer; High resolution mass spectrometric (HRMS) analyses were measured on a Finnigan MAT 95 XP spectrometer. NMR spectra were recorded on an INOVA-400 spectrometer, using TMS as an internal standard; Electronic absorption spectra were obtained on a LabTech UV Power spectrometer; Photoluminescent spectra were recorded with a HITACHI F4600 fluorescence spectrophotometer; Cell imaging was performed with a Nikon eclipse TE300 inverted fluorescence microscopy; TLC analyses were performed on silica gel plates and column chromatography was conducted over silica gel (mesh 200–300), both of which were obtained from the Qingdao Ocean Chemicals.

2.2 HeLa cell incubation and imaging using sensor Rh6G-1

HeLa cells were grown in MEM (modified Eagle's medium) supplemented with 10% FBS (fetal bovine serum) in an atmosphere of 5% CO_2 and 95% air at 37°C. The cells were plated on 6-well plates and allowed to adhere for 24 hours. Immediately before the experiments, the cells were washed with PBS buffer, and then the cells were incubated with sensor **Rh6G-1** (10 μM) and Hoechst 33258 (4.5 μM) for 30 min at 37ºC in PBS buffer (containing 1% DMSO as a cosolvent), and then washed with PBS three times. After incubating with ferric citrate (10 equiv.) for another 30 min at 37 ºC, the HeLa cells were rinsed with PBS three times, and the fluorescence images were acquired through a Nikon eclipse TE300 inverted fluorescence microscopy equipped with a cooled CCD camera.

2.3 Cytotoxicity assays

HeLa cells were grown in the modified Eagle's medium (MEM) supplemented with 10% FBS (fetal bovine serum) in an atmosphere of 5% CO_2 and 95% air at 37°C. Immediately before the experiments, the cells were placed in a 96-well plate, followed by addition of increasing concentrations of sensor **Rh6G-1** (99% MEM and 1% DMSO). The final concentrations of the sensor were kept from 5 to 200 μM (n = 3). The cells were then incubated at 37°C in an atmosphere of 5% CO_2 and 95% air at 37°C for 24 hours, respectively, followed by the standard MTT assays. An untreated assay with MEM (n = 3) was also conducted under the same conditions.

2.4 Synthesis of Compound Rh6G-1

The starting material, Rhodamine 6G hydrazide **1**, is a known compound [23] . Rhodamine 6G hydrazide **1** (800.5 mg, 1.9 mmol) and PhNCO (1200.1 mg, 10.0 mmol) in anhydrous toluene (75 mL) were heated to reflux for 1 hour. The hot solution was cooled to room temperature, and the solvent was removed under reduced pressure. The resulting residue was purified on a silica gel column (CH_2Cl_2 / petroleum = 1 : 2) to produce compound **Rh6G-1** as a white powder (249.6 mg, isolated yield: 19.7%). mp 157-159°C; ^{1}H NMR (400 MHz, $CDCl_3$): δ = 1.13-1.16 (t, 6H), 1.84 (s, 6H), 2.87-2.95 (m, 2H), 3.01-3.09 (m, 2H), 3.34 (bs, 2H), 6.26 (s, 2H), 6.38 (s, 2H), 6.95-7.01 (m, 6H), 7.12-7.16 (t, *J* = 7.8 Hz, 4H), 7.39-7.41 (d, *J* = 7.6 Hz, 1H), 7.66-7.69 (t, *J* = 7.4 Hz, 4H), 7.74-7.77 (d, *J* = 7.4 Hz, 1H), 8.09-8.11 (d, *J* = 7.2 Hz, 1H), 8.67 (bs, 2H); ^{13}C NMR (100 MHz, $CDCl_3$):14.54, 16.70, 38.17, 68.85, 96.59, 105.59, 117.57, 120.33, 123.75, 124.53, 125.05, 128.34, 129.07, 129.29, 130.39, 134.08, 137.13, 148.10, 148.57, 151.29, 153.60, 166.88; ESI-MS m/z 667.3 $[M+H]^+$; HRMS (ESI) *m/z* calcd for $C_{40}H_{39}N_6O_4$ $[M+H]^+$: 667.3027. Found 667.3013.

Synthesis of Compound RhB-2: The starting material, Rhodamine B hydrazide **2**, is a known compound [24]. Rhodamine B hydrazide **2** (100.0 mg, 0.22 mmol) and PhNCO (157.1 mg, 1.32 mmol) in anhydrous toluene (60 mL) were heated to 60 °C for 2 hours. Subsequently, the reaction mixture was heated to 110 °C and further stirred for 10 hours. The hot solution was cooled to room temperature, and the solvent was removed under reduced pressure. The resulting residue was purified on a silica gel column (petroleum ether/ CH_2Cl_2 / ethyl acetate = 3 : 2: 1) to produce compound **RhB-2** as a white powder (111.0 mg, 72.6%). mp 170-172 °C; ^{1}H NMR (400 MHz, $CDCl_3$): δ = 0.98-1.01 (t, *J* = 7.0, 12H), 3.16-3.21 (q, 8H), 6.23-6.26 (dd, *J* = 8.8,

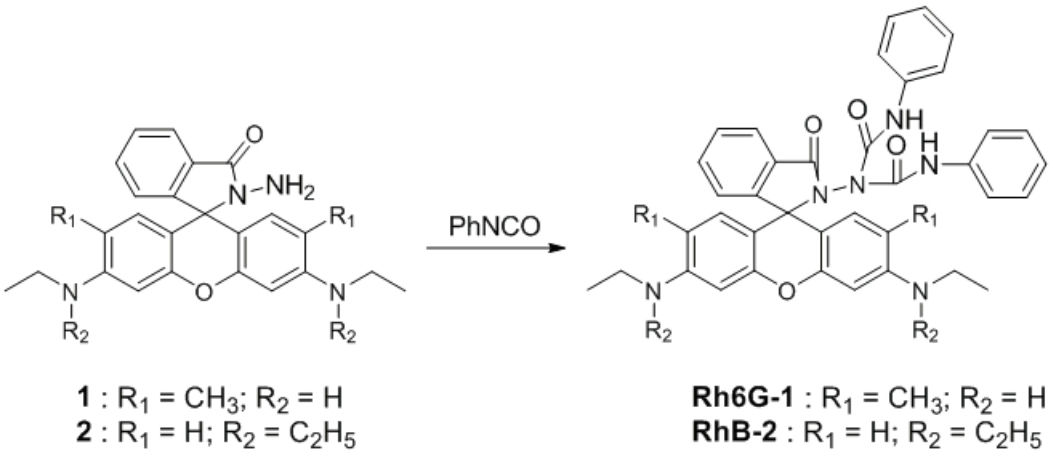

Scheme 1: Synthesis of the compounds **Rh6G-1** and **RhB-2**. Reagent and experimental condition: anhydrous toluene, reflux.

2.4 Hz, 2H), 6.32 (d, *J* = 2.4 Hz, 2H), 6.59-6.61 (d, *J* = 8.8 Hz, 2H), 6.92-6.96 (t, *J* = 7.6 Hz, 2H), 7.03-7.05 (d, *J* = 7.6 Hz, 4H), 7.09-7.13 (t, 4H), 7.42-7.44 (d, *J* = 7.6 Hz, 1H), 7.53-7.66 (t, *J* = 7.6 Hz, 1H), 7.72-7.60 (t, *J* = 7.6 Hz, 1H), 8.03-8.05 (d, *J* = 7.6 Hz, 1H), 8.76 (bs, 2H); ^{13}C NMR (100 MHz, $CDCl_3$): 12.39, 44.32, 97.75, 107.59, 120.82, 123.89, 124.56, 125.00, 128.36, 129.00, 129.47, 130.50, 133.90, 136.96, 148.21, 149.24, 151.39, 155.21, 166.92; ESI-MS m/z 695.1 $[M+H]^+$; HRMS (ESI) *m/z* calcd for $C_{42}H_{43}N_6O_4$ $[M+H]^+$: 695.3340. Found 695.3328.

Ethical approval: The conducted research is not related to either human or animal use.

3 Results and discussion

3.1 UV–vis and fluorescence spectra of sensor Rh6G-1 titrated with Fe^{3+}

Fluorescence titrations of Fe^{3+} to sensor **Rh6G-1** (10 μM) were conducted in almost pure water (containing 1% DMSO) with excitation at 500 nm at room temperature. Sensor **Rh6G-1** exhibited almost no fluorescence in water, indicating that **Rh6G-1** exists predominantly as the spirocyclic form. However, upon addition of Fe^{3+} from $FeCl_3$, the fluorescence intensity at around 556 nm significantly increases (Figure 1), and an 82-fold fluorescence enhancement was observed. The absorption titration studies are in good agreement with the turn-on fluorescence response (Figure 2). Treatment of Fe^{3+} elicited formation of an intense absorption peak at around 542 nm, indicating that sensor **Rh6G-1** is in the ring-opening form in the presence of Fe^{3+}. Notably, the sensor showed an excellent linear relationship between the fluorescence intensity at 556 nm and the concentrations of Fe^{3+} from 1 to 170 μM (Figure 3), suggesting that the sensor is potentially useful for quantitative determination of Fe^{3+}. The detection limit (S/N = 3) of sensor **Rh6G-1** was determined to be 1.2 μM in water (containing 1% DMSO) (Figure S1).

Although compound **RhB-2** may also operate as a novel fluorescent Fe^{3+} sensor in water containing 20% CH_3CN (Figure S2A), it is inferior to compound **Rh6G-1** in terms of sensitivity in water containing 1% DMSO. The fluorescence intensity of compound **RhB-2** increased from 2.7 in the absence of Fe^{3+} to 17.7 in the presence of 100 equiv. of Fe^{3+} in water (containing 1% DMSO) (Figure S2B), only a 6.6-fold fluorescence enhancement, which is much less than that (82-fold fluorescence enhancement) of compound **Rh6G-1** under the same solvent system (water containing 1% DMSO). Thus, in this work, we focused on sensor **Rh6G-1** for further studies.

3.2 Binding mode of sensor Rh6G-1 with Fe^{3+}

Job's plot according to the method for continuous variations [25] shows a 1:1 binding stoichiometry between sensor **Rh6G-1** and Fe^{3+} (Figure S3A). Based on the 1: 1 binding mode, the binding constant of sensor **Rh6G-1** in water (containing 1% DMSO as a cosolvent) was calculated as Log K_a = 3.34 from the results of the fluorescence titration experiments (Figure S3B) [26]. Importantly, the formation of sensor **Rh6G-1**/Fe^{3+} complex is prompt and reversible. The reversible nature of the interactions between **Rh6G-1** and Fe^{3+} was tested with TPEN (N, N, N', N'-Tetrakis(2-pyridylmethyl)-1, 2- ethylenediamine) which is known to bind strongly with various metal ions including Fe^{3+}. A solution of sensor **Rh6G-1** (10 μM)

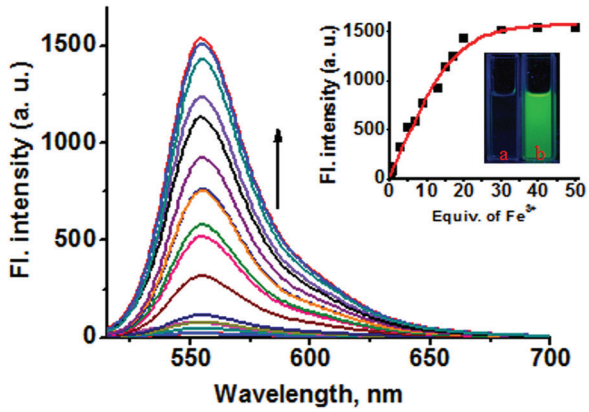

Figure 1: Fluorescence spectra of sensor **Rh6G-1** (10 μM) in the presence of increasing concentrations of Fe^{3+} (0-50 equiv.) in water (containing 1% DMSO as a cosolvent) with excitation at 500 nm. Inset: Fluorescent intensity at 556 nm of sensor **Rh6G-1** (10 μM) upon addition of Fe^{3+} (0-50 equiv.) excited at 500 nm, and the visual fluorescence color changes of the solutions a, b: a, sensor **Rh6G-1** (10 μM); b, sensor **Rh6G-1** (10 μM) + Fe^{3+} (50 eq).

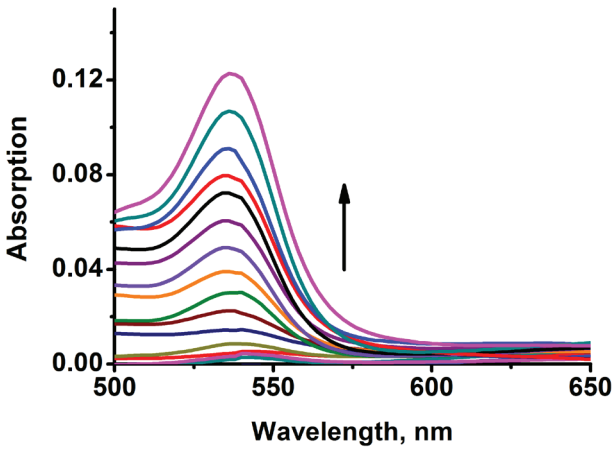

Figure 2: Absorption spectra of sensor **Rh6G-1** (10 μM) in the presence of increasing concentrations of Fe^{3+} (0 - 50 equiv.) in water (containing 1% DMSO as a cosolvent).

incubated with Fe^{3+} (10 equiv.) in water (containing 1% DMSO as a cosolvent) exhibited a strong fluorescence at around 556 nm. However, upon further titration with TPEN (0 - 60 equiv.), the fluorescence was gradually quenched (Figure 4), indicating the reversible character of the binding of sensor **Rh6G-1** with Fe^{3+}. To further test the reversible character, we carried out the cyclic tests for the reversibility of the fluorescent turn-on behavior with quenching by TPEN and followed by adding Fe^{3+} (Figure S4), the result showed that fluorescence enhancement can still be recovered after four cycles. Thus, based on these studies and the interaction mode of Fe^{3+} with the bioactive

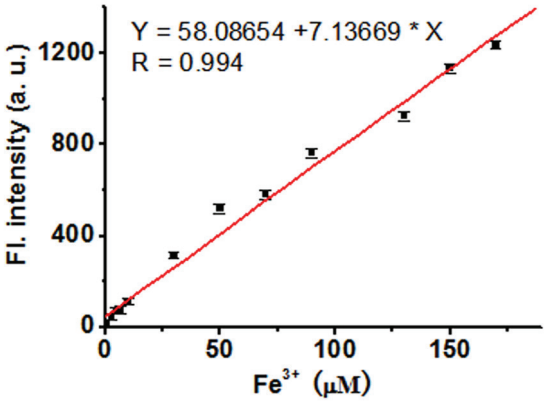

Figure 3: Plot of fluorescence intensity of sensor **Rh6G-1** (10 μM) at 556 nm vs. Fe^{3+} concentration (1 - 170 μM) in water (containing 1% DMSO as a cosolvent) excited at 500 nm.

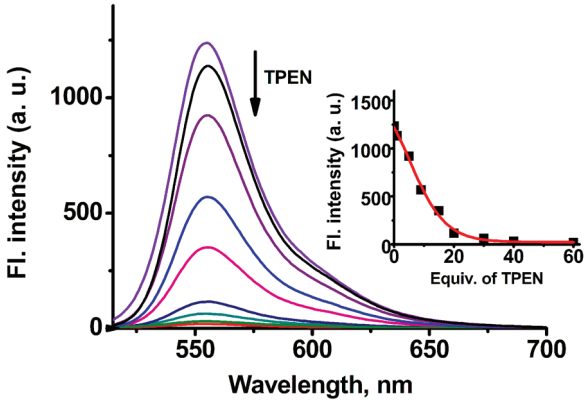

Figure 4: Fluorescence titration spectra of a solution of sensor **Rh6G-1** (10 μM) + Fe^{3+} (10 equiv.) with TPEN (0 - 60 equiv.) in water (containing 1% DMSO as a cosolvent). Inset: Fluorescent intensity at 556 nm of a solution of sensor **Rh6G-1** (10 μM) + Fe^{3+} (10 equiv.) upon addition of TPEN (0 - 60 equiv.). Excitation at 500 nm.

ferrichromes [22], a likely binding mode of sensor **Rh6G-1** with Fe^{3+} was proposed (Scheme 2).

To further understand the nature of interaction between sensor **Rh6G-1** and Fe^{3+}, the ESI-MS spectrum (positive ion mode) was carried out. The peak at m/z 667.3 (calcd 666.3) corresponded to [**Rh6G-1**+H]$^+$, when excess Fe^{3+} was added, the new highest peak was obtained at m/z 740.4 corresponded to [**Rh6G-1**+ Fe^{3+}+H_3O^+] (Figure S5), which indicated that sensor **Rh6G-1** have coordinated with Fe^{3+}. The possibility reaction mechanism was depicted in Scheme 2.

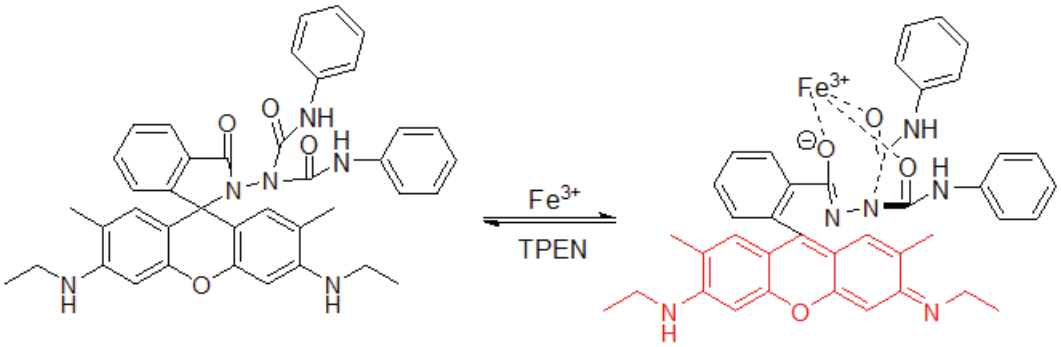

Scheme 2: The possible binding mode of sensor **Rh6G-1** with $FeCl_3$.

3.3 Selectivity studies

We then examined the selectivity of sensor **Rh6G-1** towards other metal species. The fluorescence titration experiment was carried out in water (containing 1% DMSO as a cosolvent) with a diverse array of metal species. Fluorescence data reveal that sensor **Rh6G-1** selectively responds to Fe^{3+} over various metal species tested (Figure 5). Other metal species such as Pd^{2+}, Ca^{2+}, Cd^{2+}, Co^{2+}, Zn^{2+}, Cu^{2+}, Hg^{2+}, Mg^{2+}, Mn^{2+}, Ag^{+}, Au^{3+}, Ni^{2+}, Pb^{2+}, Na^{+}, and K^{+} displayed very slighted fluorescence variations. Notably, sensor **Rh6G-1** has a high selectivity for Fe^{3+} over Fe^{2+}. We further investigated the fluorescent turn-on response of sensor **Rh6G-1** toward Fe^{3+} in the presence of other potentially competing species. The other species only exhibited minimum interference (Figure S6). This indicates that sensor **Rh6G-1** is useful to detect Fe^{3+} in the presence of other related species. Compound **RhB-2** also exhibited the high selectivity for Fe^{3+} in water containing 20% CH_3CN (Figures S7-8).

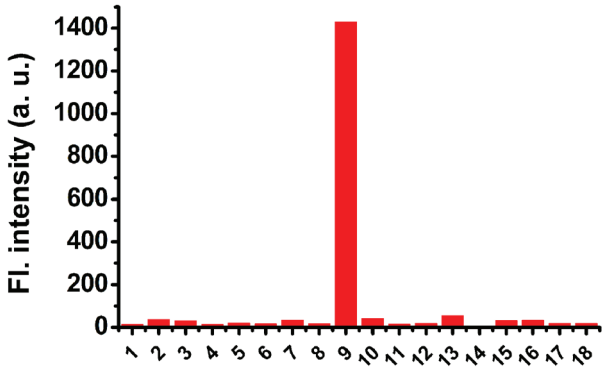

Figure 5: Fluorescence intensity changes of sensor **Rh6G-1** (10 μM) in response to various metal species (20 equiv.) in water (containing 1 % DMSO as a cosolvent). 1. none; 2. Pd^{2+}; 3. Ca^{2+}; 4. Cd^{2+}; 5. Co^{2+}; 6. Zn^{2+}; 7. Cu^{2+}; 8. Fe^{2+}; 9. Fe^{3+}; 10. Hg^{2+}; 11. Mg^{2+}; 12. Mn^{2+}; 13, Ag^{+}, 14, Au^{3+}, 15. Ni^{2+}; 16. Pb^{2+}; 17. Na^{+}, 18. K^{+}. Excitation at 500 nm; emission at 556 nm.

3.4 Effect of pH

To study the practical applicability, the effect of pH on the fluorescence response of sensor **Rh6G-1** to Fe^{3+} was investigated. As shown in Figure 6, in the absence of Fe^{3+}, almost no change in fluorescence intensity was observed in the free sensor **Rh6G-1** over a wide pH range of 4.5 - 9.0, indicating that the free sensor was stable across a wide pH range. Upon treatment with Fe^{3+}, the maximal fluorescence signal was observed in the pH range of 5.5 - 8.5. Thus, the observation that sensor **Rh6G-1** had the maximal sensing response at physiological pH, suggests that sensor **Rh6G-1** was promising for biological applications.

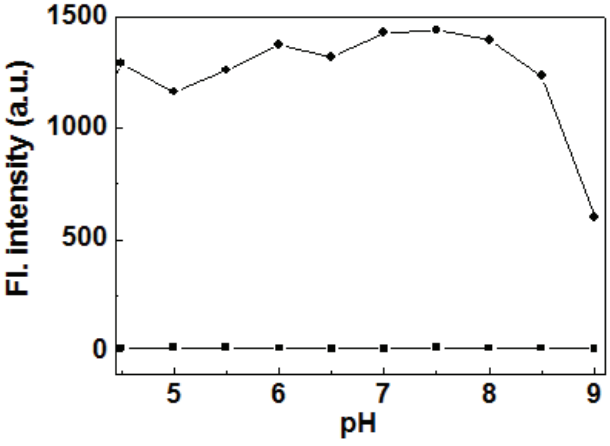

Figure 6: The fluorescence responses (at 556 nm) of free sensor **Rh6G-1** (10 μM) (■) and **Rh6G-1** (10 μM) + 20 equiv Fe^{3+} (●) in water (containing 1 % DMSO as a cosolvent) as a function of different pH values.

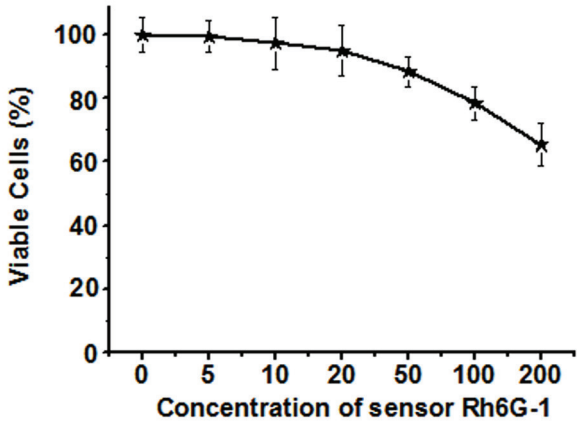

Figure 7: Cytotoxicity assay of sensor **Rh6G-1** at different concentrations (a: 0 μM; b: 5 μM; c: 10 μM; d: 20 μM; e: 50 μM; f: 100 μM; g: 200 μM) for HeLa cells.

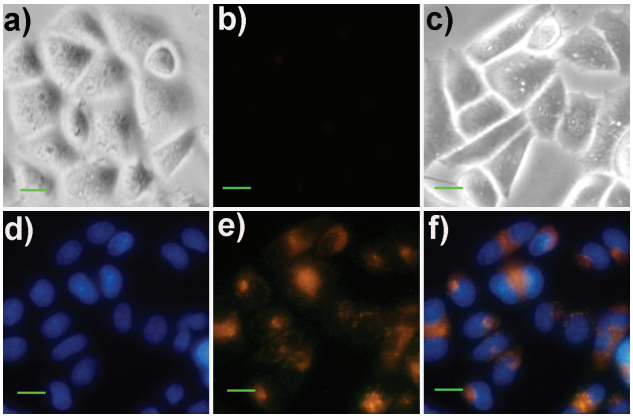

Figure 8: Bright-field and fluorescence images of HeLa cells. (a) Brightfield image of the cells treated with sensor **Rh6G-1** (10 μM) for 30 min; (b) Fluorescence image of panel (a) from the red channel; (c) Bright-field image of the cells pre-treated with sensor **Rh6G-1** (10 μM) and Hoechst 33258 (4.5 μM) for 30 min, and then incubated with Fe^{3+} (10 equiv.) for 30 min; (d) Fluorescence image of panel (c) from the blue channel; (e) Fluorescence image of panel (c) from the green/red channel; (f) Overlay of panels (d) and (e). Scale bar: 30 μm.

3.5 Fluorescence Image in Living Cells

The potential toxicity is a concern for any fluorescent sensors intended as molecular imaging agents. Thus, we set out to examine the potential toxicity of sensor **Rh6G-1** against the representative cell line, Hela cells. The living cells were incubated with various concentrations (0 - 200 μM) of the sensor for 24 h, and then the cell viability was determined by the standard 3-(4,5-dimethylthiazol-2-yl)-2,5-diphenyltetrazolium bromide (MTT) assays [27]. Almost 90% of the cells were still alive after treatment with 50 μM sensor **Rh6G-1** for 24 h (Figure 7), suggesting that sensor **Rh6G-1** has low cytotoxicity [28].

The observation that sensor **Rh6G-1** can function very well in essentially pure water renders it desirable for imaging of Fe^{3+} in living cells. To test this possibility, sensor **Rh6G-1** was incubated with the living HeLa cells. As shown in Figure 8b, the cells treated with only sensor **Rh6G-1** exhibited almost no fluorescence. However, the cells pre-loaded with sensor **Rh6G-1** and further incubated with Fe^{3+} displayed intense orange fluorescence (Figure 8e), consistent with the emission profiles of sensor **Rh6G-1** incubated with Fe^{3+} (Figure 1). Furthermore, the nuclear staining with Hoechst 33258 revealed that sensor **Rh6G-1** associates with the cytoplasm of HeLa cells (Figures 8d-f).

4 Conclusions

In conclusion, compounds **Rh6G-1** and **RhB-2** containing tri-oxygen atoms of the amide groups were designed and synthesized as new reversible fluorescent sensors for Fe^{3+}. The favorable features of the novel sensor **Rh6G-1** include a big fluorescent turn-on response in almost pure water at room temperature, high sensitivity, high selectivity, cell membrane permeability, and low cytotoxicity. These desirable attributes enable us to successfully employ the new sensor **Rh6G-1** for Fe^{3+} bioimaging in living cells. We expect that the new Fe^{3+} ligand composed of tri-oxygen atoms of the amide groups will be useful for development of a wide variety of reversible fluorescent Fe^{3+} sensors based on distinct dyes.

Acknowledgments: This work was financially supported by Hunan Provincial Key Lab of Dark Tea and Jin-hua (2016TP1022), NSFC (21502048), the Natural Science Foundation of Hunan Province (2016JJ3102), Science and Technology Innovative Research Team in Higher Educational Institutions of Hunan Province. There is no any conflict of interest in connection with this article◦ and no portion of it has been published or under consideration of publication by another journal

Conflict of interest: Authors declare no conflict of interest.

References

[1] Touati D., Iron and oxidative stress in bacteria, Arch. Biochem. Biophys., 2000, 373, 1-6.

[2] Beutler E., Felitti V., Gelbart T., Ho N., Genetics of iron storage and hemochromatosis, Drug Metab. Dispos., 2001, 29, 495-499.
[3] Andrews N.C., Disorders of iron metabolism, N. Engl. J. Med., 1999, 341, 1986-1195.
[4] Baytak S., Balaban A., Türker A.R., Erk B., Atomic absorption spectrometric determination of Fe(III) and Cr(III) in various samples after preconcentration by solid phase extraction with pyridine-2-carbaldehyde thiosemicarbazone, J. Anal. Chem., 2006, 61, 476-482.
[5] Vladescu L., Costache M., Badea I., Preparation, characterization,and metal-sorption studies of a mordant yellow 10-loaded wool, a new stable chelating material based on bleached wool, Acta Chrom., 2004, 14, 187-197.
[6] Mokgalaka N.S., Wondimu T., McCrindle R.I., Slurry nebulization ICP-OES for the determination of Cu, Fe, Mg, Mn and Zn, Bull. Chem. Soc. Ethiop., 2008, 22, 313-321.
[7] Chen X., Pradhan T., Wang F., Kim J.S., Yoon J., Fluorescent chemosensors based on spiroring-opening of xanthenes and related derivatives, Chem. Rev., 2012, 112, 1910-1956.
[8] Bricks J.L., Kovalchuk A., Trieflinger C., Nofz M., Büschel M., Tolmachev A.I., et al., On the development of sensor molecules that display Fe^{III}-amplified fluorescence, J. Am. Chem. Soc., 2005, 127, 13522-13529.
[9] Xiang Y., Tong A., A new rhodamine-based chemosensor exhibiting selective FeIII-amplified fluorescence, Org. Lett., 2006, 8, 1549-1552.
[10] Mao J., Wang L., Dou W., Tang X., Yan Y., Liu W., Tuning the Selectivity of Two Chemosensors to Fe(III) and Cr(III), Org. Lett., 2007, 9, 4567-4570.
[11] Qin J., Yang Z., Wang G., Li C., FRET-based rhodamine-coumarin conjugate as a Fe^{3+} selective ratiometric fluorescent sensor in aqueous media, Tetrahedron Lett., 2015, 56, 5024-5029.
[12] Zhao M., Deng Z., Tang J., Zhou X., Chen Z., Li X., et al., 2-(1-Pyrenyl) benzimidazole as a ratiometric and "turn-on" fluorescent probe for iron(III) ions in aqueous solution, Analyst, 2016, 141, 2308-2312.
[13] Ma S., Yang Z., She M., Sun W., Yin B., Liu P., et al., Design and synthesis of functionalized rhodamine based probes for specific intracellular fluorescence imaging of Fe^{3+}, Dyes Pigm., 2015, 115, 120-126.
[14] Hu Z.Q., Du M., Zhang L.F., Guo F.Y., Liu M.D., Li M., A novel colorimetric and fluorescent chemosensor for cyanide ion in aqueous media based on a rhodamine derivative in the presence of Fe^{3+} ion, Sens. Actuators, B, 2014, 192, 439-443.
[15] Zhou F., Leng T.H., Liu Y.J., Wang C.Y., Shi P., Zhu W.H., Water-soluble rhodamine-based chemosensor for Fe^{3+} with high sensitivity, selectivity and anti-interference capacity and its imaging application in living cells, Dyes Pigm.., 2017, 142, 429-436.
[16] Wang K., Lei Y., Zhang S., Zheng W., Chen J., Chen S., et al., Fluorescent probe for Fe(III) with high selectivity and its application in living cells, Sens. Actuators, B, 2017, 252, 1140-1145.
[17] Yan F., Zheng T., Shi D., Zou Y., Wang Y., Fu M., et al., Rhodamine-aminopyridine based fluorescent sensors for Fe^{3+} in water: Synthesis, quantum chemical interpretation and living cell application, Sens. Actuators, B, 2015, 215, 598-606.
[18] Lee M.H., Giap T.V., Kim S.H., Lee Y.H., Kang C., Kim J.S., A novel strategy to selectively detect Fe(III) in aqueous media driven by hydrolysis of a rhodamine 6G Schiff base, Chem. Commun., 2010, 46, 1407-1409.
[19] Kim H.N., Lee M.H., Kim H.J., Kim J.S., Yoon J., A new trend in rhodamine-based chemosensors: application of spirolactam ring-opening to sensing ions, Chem. Soc. Rev., 2008, 37, 1465-1472.
[20] Beija M., Afonso C.A.M., Martinho J.M.G., Synthesis and applications of Rhodamine derivatives as fluorescent probes, Chem. Soc. Rev., 2009, 38, 2410-2433.
[21] Chen X., Wang F., Hyun J.Y., Wei T., Qiang J., Ren X., et al., Recent progress in the development of fluorescent, luminescent and colorimetric probes for detection of reactive oxygen and nitrogen species, Chem. Soc. Rev., 2016, 45, 2976-3016.
[22] Nudelman R., Ardon O., Hadar Y., Chen Y., Libman J., Shanzer A., Modular fluorescent-labeled siderophore analogues, J. Med. Chem., 1998, 41, 1671-1678.
[23] Yang Y.K., Yook K.J., Tae J., A rhodamine-based fluorescent and colorimetric chemodosimeter for the rapid detection of Hg^{2+} ions in aqueous media, J. Am. Chem. Soc., 2005, 127, 16760-16761.
[24] Xiao X.F., Guo X.Q., Zhao Y.B., Development of a novel rhodamine type fluorescent probe to determine peroxynitrite, Talanta, 2002, 57, 883-890.
[25] Vosburgh W.C., Cooper G.R., Complex ions. I. The identification of complex ions in solution by spectrophotometric measurements, J. Am. Chem. Soc., 1941, 63, 437-442.
[26] Ho I.T., Lee G.H., Chung W.S., Synthesis of upper-Rim allyl- and p-methoxyphenylazocalix[4]arenes and their efficiencies in chromogenic sensing of Hg^{2+} Ion, J. Org. Chem., 2007, 72, 2434-2442.
[27] Mosmann T., Rapid colorimetric assay for cellular growth and survival: Application to proliferation and cytotoxicity assays, J. Immunol. Methods, 1983, 65, 55-63.
[28] Wang J., Long L., Xiao X., A Fast-responsive Fluorescent Probe for Sulfite and Its Bioimaging, Luminescence, 2016, 32, 775-781.

Supplemental Material: The online version of this article offers supplementary material (https://doi.org/10.1515/chem-2018-0140).